Molecular Biology of the Cell
Vol. 14, 4857–4870, December 2003

Human Immunodeficiency Virus-1 Nef Expression Induces Intracellular Accumulation of Multivesicular Bodies and Major Histocompatibility Complex Class II Complexes: Potential Role of Phosphatidylinositol 3-Kinase

Pamela Stumptner-Cuvelette,* Mabel Jouve, Julie Helft, Marc Dugast, Anne-Sophie Glouzman,† Karin Jooss,‡ Graça Raposo,† and Philippe Benaroch*§

*Institut National de la Santé et de la Recherche Médicale U520 and †Centre National de la Recherche Scientifique Unité Mixte Recherche 144, Institut Curie, Section de recherche. 75005 Paris, France; and ‡Genethon III, 91002 Evry, France

Submitted April 8, 2003; Revised August 1, 2003; Accepted August 22, 2003
Monitoring Editor: Juan Bonifacino

Nef alters the cell surface expression of several immunoreceptors, which may contribute to viral escape. We show that Nef modifies major histocompatibility complex class II (MHC II) intracellular trafficking and thereby its function. In the presence of Nef, mature, peptide-loaded MHC II were down-modulated at the cell surface and accumulated intracellularly, whereas immature (invariant [Ii] chain-associated) MHC II expression at the plasma membrane was increased. Antibody internalization experiments and subcellular fractionation analyses showed that immature MHC II were internalized from the plasma membrane but had limited access to lysosomes, explaining the reduced Ii chain degradation. Immunoelectron microscopy revealed that Nef expression induced a marked accumulation of multivesicular bodies (MVBs) containing Nef, MHC II, and high amounts of Ii chain. The Nef-induced up-regulation of surface Ii chain was inhibited by LY294002 exposure, indicating the involvement of a phosphatidylinositol 3-kinase, whose products play a key role in MVB biogenesis. Together, our results indicate that Nef induces an increase of the number of MVBs where MHC II complexes accumulate. Given that human immunodeficiency virus recruits the MVB machinery for its assembly process, our data raise the possibility that Nef is involved in viral assembly through its effect on MVBs.

INTRODUCTION

The *nef* gene is highly conserved in primate lentiviruses and expressed abundantly in the early stages and throughout the viral replication cycle. Despite its small size, the Nef protein has been credited with a remarkable number of distinct functions. In vivo studies showed Nef to be a key component in human immunodeficiency virus (HIV) pathogenesis (Kestler *et al*., 1991; Hanna *et al*., 1998a,b). However, the underlying cellular and molecular mechanisms of its contribution to disease progression and pathogenesis remain elusive. Nef also enhances virion infectivity and viral production (Miller *et al*., 1994; Spina *et al*., 1994; Schwartz *et al*., 1995; Dorfman *et al*., 2002). This phenomenon is possibly related to one of the best characterized functions of Nef, the down-regulation of the CD4 cell surface receptor by a posttranslational mechanism (Garcia and Miller, 1991; Aiken *et al*., 1994; Lundquist *et al*., 2002). The reduction in cell surface CD4 facilitates viral release by preventing sequestration of the HIV gp120 protein through CD4 and increases the infectivity of viral particles (Lama *et al*., 1999; Ross *et al*., 1999).

Nef interferes with the immune system by disrupting antigen recognition at different levels. In addition to the accelerated endocytosis of CD4, part of the T cell receptor machinery, Nef also enhances internalization of the costimulatory CD28 molecule, impeding effective T cell activation (Swigut *et al*., 2001). Furthermore, Nef induces apoptosis of virus-specific cytotoxic T-lymphocytes via expression of CD95L, while protecting infected cells by modifying the signal transduction pathway regulating apoptosis (Fackler and Baur, 2002). This modification involves a phosphatidylinositol 3-kinase (PI 3-kinase) and a p21-activated kinase, which are both bound and activated by Nef in a sequential manner (Wolf *et al*., 2001). The fate of cell surface major histocompatibility complex (MHC) class I is also altered in Nef-expressing or HIV-infected cells, leading to HLA-A and -B sequestering in perinuclear compartments (Schwartz *et al*., 1996; Greenberg *et al*., 1998; Le Gall *et al*., 1998). Nef induces, together with PACS-1, MHC I endocytosis from the plasma membrane to the *trans*-Golgi network (TGN) through the PI3 kinase-mediated ARF6 endosomal pathway (Piguet *et al*., 2000; Blagoveshchenskaya *et al*., 2002). The reduced density of HLA-A and -B at the cell surface may allow infected cells to escape recognition and lysis by virus specific $CD8^+$ T cells (Collins *et al*., 1998; Collins and Baltimore, 1999). Interestingly the surface expression of HLA-C is not modified,

Article published online ahead of print. Mol. Biol. Cell 10.1091/mbc.E03–04–0211. Article and publication date are available at www.molbiolcell.org/cgi/doi/10.1091/mbc.E03–04–0211.

§ Corresponding author. E-mail address: benaroch@curie.fr or graposo@curie.fr.

Abbreviations used: EM, electron microscopy; HA, hemagglutinin; Ii, Ii chain; MFI, mean fluorescence intensity; MHC, major histocompatibility complex; MVB, multivesicular body; PI 3-kinase, phosphatidylinositol 3-kinase; TfR, transferrin receptor; TGN, *trans*-Golgi network.

protecting infected cells from lysis by NK cells (Le Gall *et al*., 1998; Cohen *et al*., 1999). Infection of rhesus macaques with simian immunodeficiency virus carrying a point mutation in its *nef* gene that selectively disrupts MHC I down-regulation resulted in rapid reversion to wild-type *nef*, indicating a strong selective advantage of Nef-mediated MHC I down-regulation for viral replication in vivo (Munch *et al*., 2001).

In the presence of Nef, we demonstrated an increase in the cell surface expression of invariant (Ii) chain-associated, and therefore nonfunctional, MHC II. In contrast, the cell surface expression of peptide-loaded mature MHC II was reduced (Stumptner-Cuvelette *et al*., 2001). We also showed that up-regulation of surface Ii chain complexes requires lower amounts of Nef than the down-regulation of mature MHC II and that both functions are genetically separable. A recent study has confirmed these results and further shows that both activities are well conserved among *nef*-alleles from primary HIV-1, HIV-2, and simian immunodeficiency virus (Schindler *et al*., 2003). Importantly, Ii surface up-regulation was observed for *nef*-alleles derived from all progressing HIV-1–infected individuals studied but for two of four long-term nonprogressors (Schindler *et al*., 2003). This suggests that this function of Nef participates to viral immune escape in vivo. Indeed, HIV-specific helper T cell responses are impaired in progressing HIV-1–infected individuals and are strong in long-term nonprogressors (Rosenberg *et al*., 1997; Pitcher *et al*., 1999). The capacity of Nef to affect MHC II antigen presentation and therefore the generation of virus-specific T cell help may be important for the control of the infection. To achieve their function of antigen presentation, MHC II traffic through a specific intracellular pathway. Newly synthesized MHC II is made of α and β chains, which associate with the Ii chain in the endoplasmic reticulum. The $\alpha\beta$Ii complexes have to traffic through the Golgi apparatus and the endocytic pathway to undergo complete maturation before presenting their antigenic peptide cargo at the cell surface (Hiltbold and Roche, 2002). During this journey, the associated Ii chain is degraded in a sequential manner, and Ii and its fragments drive associated $\alpha\beta$ complexes to specialized endocytic compartments, where peptides are loaded onto MHC II (Stumptner-Cuvelette and Benaroch, 2002).

Here, we show that Nef impedes MHC II function through a novel posttranslational mechanism modifying the MHC II intracellular trafficking. Nef expression led to an increased access of $\alpha\beta$Ii complexes at the cell surface and an impairment of the degradation of the Ii chain. We observed by electron microscopy (EM) that Nef expression induced a striking increase in the number of multivesicular bodies (MVBs) in two different cell lines. These structures contained MHC II and large amounts of apparently intact Ii chain. The Nef-induced up-regulation of Ii chain was dependent on a PI 3-kinase activity, which could be recruited and activated by Nef at the MVB level as Nef seemed enriched at the MVB outer membrane. Because phosphoinositides are involved in MVB biogenesis, the Nef-induced increase of MVB numbers might be related to the PI 3-kinase activation. Our results indicate that Nef affects transport of immature MHC II complexes ($\alpha\beta$Ii) to lysosomal compartments, which rather accumulate in MVBs and at the plasma membrane.

MATERIALS AND METHODS

Antibodies

The following anti-HLA-DR antibodies were used: a rabbit polyclonal anti–HLA-DR kindly provided by H.L. Ploegh (Harvard Medical School, Cambridge, MA), the monoclonal antibody (mAb) TU36 (Shaw *et al*., 1985), the mAb L243 (Lampson and Levy, 1980), and the mAb 1B5 (Adams *et al*., 1983). ICC5 and ICN1 antibodies specific for the C-terminal and N-terminal domains of the Ii chain, respectively, have been generated by P. Morton (Monsanto, St. Louis, MO) and were used for immuno-EM. A rabbit immunesera directed against Ii (Salamero *et al*., 1996), and three Ii chain-reactive mouse mAbs were also used: PIN1 (Lamb and Cresswell, 1992) directed against the N terminus of Ii, BU45 (Wraight *et al*., 1990) and LN-2 (BD PharMingen, San Diego, CA) directed against the lumenal part of Ii. In addition, we used mAb W6/32 (Parham *et al*., 1979) that recognizes mature MHC I complexes, mAb 66Ig10 (van de Rijn *et al*., 1983) directed against the human transferrin receptor (TfR), mAb MATG 020 directed against Nef, mAb H37/38 directed against hemagglutinin (HA) (Sarukhan *et al*., 2001), mAb anti-Lamp-1 from BD PharMingen, and an IgG1 mAb anti-CD63 clone CLB-gran (Caltag Laboratories, Burlingame, CA), a sheep immunesera anti-TGN46 (kind gift of V. Ponnambalam, University of Dundee, Dundee, United Kingdom). Secondary antibodies were from Jackson ImmunoResearch Laboratories (West Grove, PA).

Plasmids

We used cytomegalovirus-driven vectors carrying the *nef* gene from *LAI*: Nef-FT (Bachelerie *et al*., 1990), a control plasmid Nef-mock carrying the *nef* A01 gene in an antisense orientation (Le Gall *et al*., 1998).

Cell Culture

HeLa and HeLa-CIITA cells (Stumptner-Cuvelette *et al*., 2001) and Mel JuSo cells were cultured in DMEM containing 4.5 g glucose/l (Invitrogen, Paisley, Scotland) supplemented with 10% fetal calf serum (Dutscher, Brumath, France), 2 mM glutamine, penicillin/streptomycin (100 IU/ml and 100 μg/ml, respectively), 1 mM sodium pyruvate, and 1% nonessential amino acids. HeLa-CIITA cells were grown in the presence of 300 μg/ml hygromycin B (Calbiochem, La Jolla, CA).

Transfections and Infections

For transient transfection experiments, cells were electroporated using a Bio-Rad gene pulser II as described previously (Stumptner-Cuvelette *et al*., 2001). Briefly, 8×10^6 cells were transfected at 200 V and 975 μF with up to 25 μg of the different expression vectors mixed with 1 μg of pEGFP and completed with the pSP72 plasmid to reach a total of 30 μg of DNA per electroporation. Two recombinant adenoviral vectors were used. rAd-HA codes for the influenza virus HA has been described previously (Sarukhan *et al*., 2001). For the generation of rAd-Nef-IRES-HA, *nef* was isolated from pSP73-Nef (kindly provided by O. Schwartz, Pasteur Institute, Paris, France) by *Sal*I/*Eco*RI digestion and cloned into the *Xho*I/*Sal*I sites of pIRESeGFP (BD Biosciences Clontech, Palo Alto, CA). The eGFP sequence from pIRESeGFP was excised by *Bst*XI/*Not*I digestion and replaced by a polylinker harboring the following sites: *Bst*XI-*Spe*I-PmeI-*Pvu*I-*Not*I, resulting in NEF-IRES-mcs. The HA cDNA was isolated from HApcDNA3 (kindly provided by D. Pardoll, Johns Hopkins School of Medicine, Baltimore, MD) and cloned into the *Spe*I/*Not*I sites of NEF-IRES-mcs. The NEF-IRES-HA cassette was excised by *Nhe*I/*Not*I and cloned into the same sites in pTG6600 (Transgene, Strasbourg, France). The E1-deleted rAd-NEF-IRES-HA vector was generated via homologous recombination as described previously (Chartier *et al*., 1996).

Flow Cytometry

For surface staining cells were detached 24 h after transfection and stained with various mouse mAbs in phosphate-buffered saline (PBS) containing 3% fetal calf serum and 0.05% azide on ice. Phycoerythrine (PE)-conjugated goat anti-mouse $F(ab)'_2$ fragments were used as secondary reagents. Dead cells were excluded by a gate in foward light scatter/standard saline citrate. Events corresponding to at least 3000 live cells positive for green fluorescent protein (GFP) were accumulated per sample. Flow cytometry analysis was performed with a FACScan using CellQuest software (BD Biosciences, Mountain View, CA).

For permeabilized fluorescence-activated cell sorting (FACS) experiments cells were detached 24 h after transfection, fixed with 1% paraformaldehyde, before quenching with 0.1 M glycine in PBS, and permeabilizing the cells in PBS, 0.2% bovine serum albumin (BSA), 0.05% saponin. Cells were then stained as described above except that the permeabilization buffer was used for dilution of the antibodies and all washing steps.

Internalization experiments were performed with cells recovered 24 h after transfection and incubated in parallel with LN-2 and 66Ig10 mAbs for 30 min on ice. The cells were then washed in ice-cold PBS and incubated at 37°C in complete medium supplemented with 20 mM HEPES for different periods of time. Antibodies remaining at the cell surface were revealed with PE-conjugated anti-mouse $F(ab)'_2$ fragments. Samples were analyzed with a FACScan as described above. Mean fluorescence intensity (MFI) of FL2 on GFP^+ cells, from which the background value obtained with a control mAb was deduced, was plotted as a function of time.

Pulse-Chase Analysis, Cell Surface Biotinylation, and Immunoprecipitation

Twenty-four hours after transfection cells were detached, washed, and starved in RPMI met$^-$cys$^-$ supplemented with 2 mM L-glutamine and 20 mM HEPES for 45 min at 37°C. Cells were then pulsed for 15 min at 0.5 mCi/ml before incubation in complete RPMI supplemented with 1 mM L-methionine for different periods of time. At the end of the chase, cells were biotinylated for 5 min with NHS-SS-biotin (2 mg/ml in PBS at 4°C; Pierce Chemical, Rockford, IL). Lysis and immunoprecipitations were carried out as described previously (Benaroch *et al*., 1995). Ten percent of the eluate was kept for subsequent SDS-PAGE analysis (total molecules), and the remaining 90% was incubated with strepavidin-agarose beads (Pierce Chemical) to precipitate the biotinylated fraction. All samples were run on 12% polyacrylamide-SDS gels, analyzed by autoradiography, and quantified with a PhosphorImager (Amersham Biosciences, Piscataway, NJ) by using the ImageQuant software.

Immunofluorescence Microscopy

Cells (1×10^5) were seeded immediately after transfection on glass coverslips in 24-well plates and allowed to adhere for 24 h. Rabbit anti-Ii immune serum, LN-2 mAb, or as a control the irrelevant mAb 9E10 were internalized for 1 h at 19.5°C and then chased for 90 min at 37°C. Lysosomes were identified by incubating the cells during 90 min with LysoTracker Red DND99 (Molecular Probes, Eugene, OR) at 37°C. All subsequent steps were carried out at room temperature. Cells were fixed for 30 min with 4% (wt/vol) paraformaldehyde in PBS followed by quenching with 0.1 M glycine in PBS. Permeabilization and saturation were performed in PBS containing 0.2% BSA and 0.05% (wt/vol) saponin. Primary antibodies were incubated for 1 h. Secondary antibodies coupled to fluorescein isothiocyanate (FITC), Cy-3, or Cy-5 were allowed to bind for 30 min. The coverslips were mounted with Mowiol on glass slides and analyzed using a TCS4D scanning laser confocal microscope (Leica Microscopy and Scientific Instruments, Heerbrugg, Switzerland). Uptake of the irrelevant 9E10 mAb gave only very faint staining showing that given the low mAb concentration used (1 μg/ml), uptake by fluid phase endocytosis was neglectable compared with uptake through Ii chain endocytosis. For conventional microscopy, cells were fixed, permeabilized, and stained as described above. Images were captured using a 100× oil immersion objective on a Leica DMRB microscope using a Nikon ACT-1 version 2.00 software.

Subcellular Fractionation

Cells (16×10^6) in 3.2 ml of 1% fetal calf serum in DMEM were infected with Ad-HA or with Ad-Nef-IRES-HA with a multiplicity of infection of 75 infectious viral particles for 90 min followed by two washes in PBS. Twenty-four hours after infection, cells were detached, washed, and subjected to subcellular fractionation, adapted from Bonnerot *et al*. (1998). In brief, 3×10^7 cell/ml were incubated in 1× tetraethylammonium (TEA) buffer (10 mM triethanolamine, 1 mM EDTA, 10 mM acetic acid, 250 mM sucrose, pH 7.4) during 10 min at 0°C. Cells were then disrupted in presence of 1 mM phenylmethylsulfonyl fluoride by a ball-bearing homogenizer at 0°C. Nuclei were eliminated by two sequential centrifugations of 7 min at $1600 \times g$. Protein contents of postnuclear supernatants were determined with a Bradford test and for each cell population, the same amount of proteins was added under a volume of 400 μl in 1× TEA buffer to a mix of Percoll at 90% in 10× TEA buffer (1.6 ml) and 3.1 ml of 1× TEA buffer, in a Beckman Quick Seal centrifuge tube. Tubes were ultracentrifuged for 35 min at 4°C at $33{,}000 \times g$. 16 fractions of 300 μl were harvested from which Percoll was eliminated by a NaOH precipitation before analysis by Western blotting for their contents in TfR, Erp57, HLA-DMβ, HLA-DRα, Ii, and Lamp-1. Anti-immunoglobulin secondary antibodies (Jackson ImmunoResearch Laboratories) used to reveal these proteins were coupled to alkaline phosphatase, whose activity was measured with ECF substrate (Amersham Biosciences) allowing quantification on a PhosphorImager (Amersham Biosciences) by using the ImageQuant software. In addition, β-hexosaminidase activity was directly measured in the fractions as follows: 40 μl of each fraction was mixed with 12 μl of substrate 10× (4-methyl-umbelliferyl-*N*-acetyl-β-D-glucosaminide; Sigma-Aldrich, St. Louis, MO) and 60 μl of 2× buffer (22.4 mM acid citric, 35.2 mM Na_2HPO_4, pH 4.5, 0.2% Triton X-100). After 3 h of incubation at 37°C, the reaction was read on a multiplate reader (Victor, Wallac, Finland) at 355 nm.

Immunoelectron Microscopy

HeLa-CIITA cells were recovered 24 h after transfection and fixed with a mixture of 2% paraformaldehyde and 0.125% glutaraldehyde in 0.2 M phosphate buffer pH 7.4 for 2 h at room temperature. Mel JuSo cells were infected with Ad-HA or with Ad-Nef-IRES-HA as described for subcellular fractionation experiments. Twenty-four hours after infection, cells were recovered and processed as described above. Fixed cells were processed for ultrathin sectioning and immunolabeling as described previously (Raposo *et al*., 1997). Quantification of the numbers of MVBs and lysosomes in both Nef-expressing cells and mock-transfected HeLa-CIITA cells was directly performed under the electron microscope. Similar quantifications were achieved in Mel JuSo cells infected with Ad-HA or with Ad-Nef-IRES-HA. In each case, 30 profiles of ultrathin-cryosectionned cells, randomly taken, were analyzed.

For analyzing the uptake and transport of a fluid phase marker of endocytosis HeLa-CIITA cells were recovered 24 h after transfection, washed once in RPMI, and then incubated with BSA coupled to 5-nm colloidal gold particles (OD_{520} = 5) for 90 min at 37°C in RPMI before fixing the cells and proceeding as described above.

Inhibition of PI 3-Kinase

HeLa-CIITA cells transfected 24 h earlier with Nef-FT or Nef-mock, and pEGFP were processed for either flow cytometry or immunofluorescence. For flow cytometry analysis, the last 15 h of transfection cells were incubated with 50 μM LY294002 (BIOMOL Research Laboratories, Plymouth Meeting, PA) or its solvent, dimethyl sulfoxide (DMSO). For immunofluorescence, the inhibitor or its solvent were added during the last 3 h of transfection.

RESULTS

Nef Expression Slows Down Ii Chain Degradation by a Posttranslational Mechanism

To investigate MHC II biosynthesis and transport in the presence of Nef, pulse-chase analysis of MHC II were carried out on HeLa-CIITA cells transfected with Nef-FT or Nef-mock as a control. After a 15-min pulse identical levels of Ii, DRα and β were immunoprecipitated from cells expressing Nef and from control cells (Figure 1A, see 0-h chase lanes and the corresponding histogram). Similar results were obtained in another cell system with a shorter 5-min pulse. This suggests that Nef does not affect the rate of synthesis of Ii, DRα, and β chains. However, degradation of the Ii chain was slower in cells expressing Nef than in control cells, because both DRα and Ii immunoprecipitates contained higher amounts of Ii chain at 4, 8, and 22 h of chase than in control cells in which Ii was hardly detectable at the 8-h chase point (Figure 1A, DRα [95°C] and Ii, and the histogram of Ii quantification).

Depending on the DR alleles, $\alpha\beta$Ii can remain stable in SDS at room temperature, generating complexes of apparent molecular mass of ~100 kDa, which dissociate upon boiling (Stumptner and Benaroch, 1997). Such complexes were observed in immunoprecipitates performed with 1B5, an anti-DRα mAb (Figure 1) or with PiN1, an anti-Ii mAb when eluted at room temperature. Therefore, these SDS-stable complexes were in all likelihood $\alpha\beta$Ii complexes. They clearly stayed associated for longer time in the presence of Nef [Figure 1A, DRα (RT); see arrowhead]. This indicated that the pool of Ii chain, which was degraded more slowly in the presence of Nef, remained associated with DR molecules. The disappearance of $\alpha\beta$Ii was accompanied by the appearance of SDS-stable $\alpha\beta$ complexes, representative of a peptide-loaded state [Figure 1A, DRα (RT); see arrowhead and star, respectively]. Quantification of these peptide-loaded SDS-stable complexes at the different chase times gave rise to only slightly reduced values in Nef-FT versus Nef-mock transfected cells (our unpublished data). This may be due in part to the chase times chosen, which may prevent visualization of a delay in the appearance of mature MHC II. In addition, Nef expression led to only a twofold reduction of the surface level of mature MHC II (Stumptner-Cuvelette *et al*., 2001). To control the experimental conditions, TfR was sequentially immunoprecipitated from the supernatants of Ii chain immunoprecipitations. The levels of synthesis, the rate of acquisition of complex sugars and the degradation of this receptor were very similar in both cell populations (Figure 1A, TfR panel and corresponding histogram), suggesting that the secretory pathway was not affected by Nef expression.

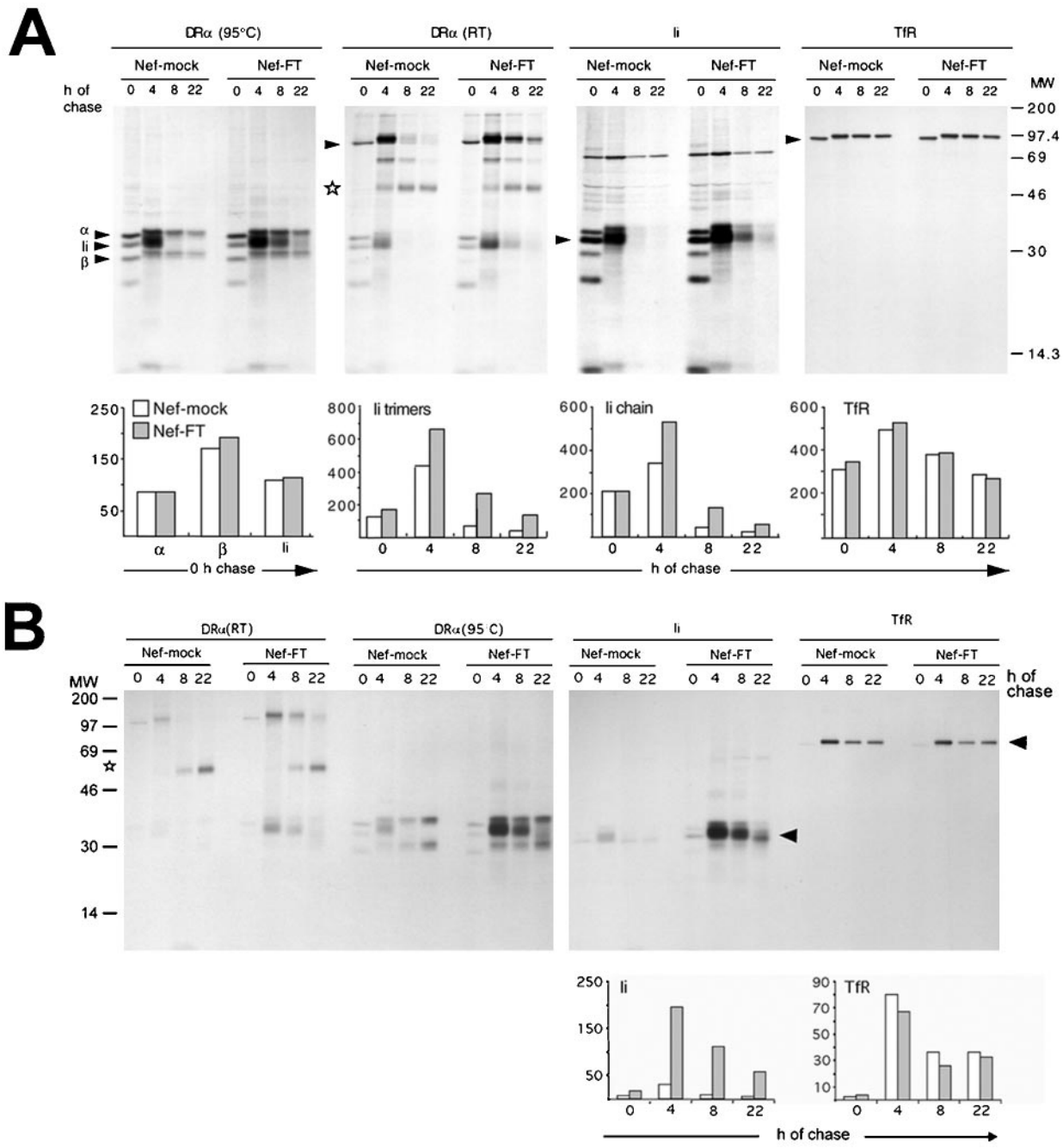

Figure 1. Nef reduces Ii chain degradation. HeLa-CIITA cells transfected with Nef-FT or Nef-mock were pulse-labeled with ^{35}S-met and -cys for 15 min and chased for 0, 4, 8, or 22 h. At the end of the chase cells were surface-biotinylated before lysis and immunoprecipitation with PIN1 (anti-Ii chain), 1B5 (anti-DRα), or 66Ig10 (anti-TfR) mAbs. (A) Immunoprecipitates eluted at 95°C or in the case of the DRα (RT) panel at room temperature, were analyzed by SDS-PAGE. Quantification by phosphorimage analyses of the indicated chains or complexes (see arrowheads) are represented as histograms below the gels (arbitrary units). Ii trimers designate $\alpha\beta$Ii complexes. (B) The biotinylated fraction of the immunoprecipitated molecules analyzed in A were reprecipitated with streptavidin-agarose beads and analyzed by SDS-PAGE. Therefore the streptavidin-precipitated material represents molecules expressed at the cell surface.

To investigate surface access of the proteins of interest, our pulse-chase experiments included a cell surface biotinylation step before cell lysis. The biotinylated fraction of the immunoprecipitated molecules was further reprecipitated with streptavidin-agarose beads. Under these conditions, streptavidin-precipitated material exclusively represents cell surface-expressed molecules. Whereas both cell populations contained similar total levels of $\alpha\beta$Ii complexes after 4 h of chase (Figure 1A, DRα and Ii), a much larger fraction of these complexes had reached the cell surface in the case of Nef expressing cells (Figure 1B; see corresponding panels). Ii chain at the cell surface remained associated with MHC II

chains (Figure 1B). In Nef-expressing cells, the disappearance of the total population of αβIi complexes paralleled the situation observed at the cell surface (compare Ii histograms Figure 1, A and B). This disappearance was concomitant with the appearance at the cell surface of SDS-stable αβ-peptide complexes whose production was not significantly altered by Nef (Figure 1B). The transport kinetics of the TfR to the cell surface remained similar in both cell types (Figure 1B).

We conclude that expression of Nef does not affect the synthesis of MHC II and Ii but reduces the rate of degradation of Ii associated to MHC II. Newly synthesized αβIi complexes accumulate at the cell surface in the presence of Nef, but neither the formation nor the transport to the cell surface of mature MHC II are significantly impaired.

Nef Induces Intracellular Accumulation of Mature MHC II

Next, the effect of Nef expression on intracellular versus surface MHC II levels was evaluated. HeLa-CIITA cells cotransfected with pEGFP and either Nef-FT or Nef-mock were analyzed by FACS analysis for cell surface staining on intact cells and total staining on permeabilized cells. Note that MFI values obtained on permeabilized cells cannot be directly compared with those obtained with intact cells due to the permeabilization procedure, which partially affects the surface levels. Although Nef reduced surface levels of mature MHC II by 50%, total levels of mature MHC II were not affected by Nef (Figure 2A). This indicated that Nef expression induced an intracellular accumulation of mature MHC II. Similar conclusions could be drawn from our data regarding MHC I (Figure 2A) in accordance with the Nef-induced accumulation of MHC I observed at the Golgi level (Le Gall *et al.*, 1998; Piguet *et al.*, 2000). Surface and total levels of Ii chain as detected with a mAb specific for the Ii lumenal domain were significantly increased in Nef-expressing cells. Therefore, the increase of total Ii chain might reflect at least in part the increase of surface Ii chain but may also mean that Ii containing complexes accumulate intracellularly.

Because more αβIi complexes seemed to gain access to the cell surface in the presence of Nef, their fate was investigated in normal HeLa-CIITA cells and in cells transfected with Nef-FT or Nef-mock. Cells exposed to 20 nM ConB (concanamycin B) overnight were used as a positive control for surface Ii chain expression, because this potent v-ATPase inhibitor induces expression of αβIi complexes at the surface of Epstein-Barr virus-transformed B cells (Benaroch *et al.*, 1995). The various cell populations were incubated on ice with LN2, a mAb specific for the lumenal side of the Ii chain. After washing, cells were shifted to 37°C for various lengths of time and then fixed and stained with secondary antibodies specific for mouse IgG. As described above, transfected cells were identified and gated on the basis of their GFP expression. In Nef-expressing cells, 50% of the surface bound Ii mAb was removed within 20 min, whereas the kinetics observed in ConB-treated cells was slightly slower (Figure 2B). Disappearance of surface bound anti-Ii mAb correlated with its intracellular appearance by confocal microscopy (see below). Low levels of surface Ii expressed on control cells (either Nef-mock transfected cells or nontransfected cells) prevented accurate determination of the uptake (Figure 2B). As a control, we followed the fate of a surface bound mAb specific for the TfR, which was rapidly internalized in both cell populations (80% in 10 min), in agreement with previous studies showing that Tf uptake was not affected by Nef expression in T cells (Foti *et al.*, 1997) and in HeLa cells (Johannes *et al.*, 2003). These data together with the pulse-chase surface biotinylation experiments (Figure 1B) suggest that in Nef-expressing cells, surface αβIi complexes are internalized.

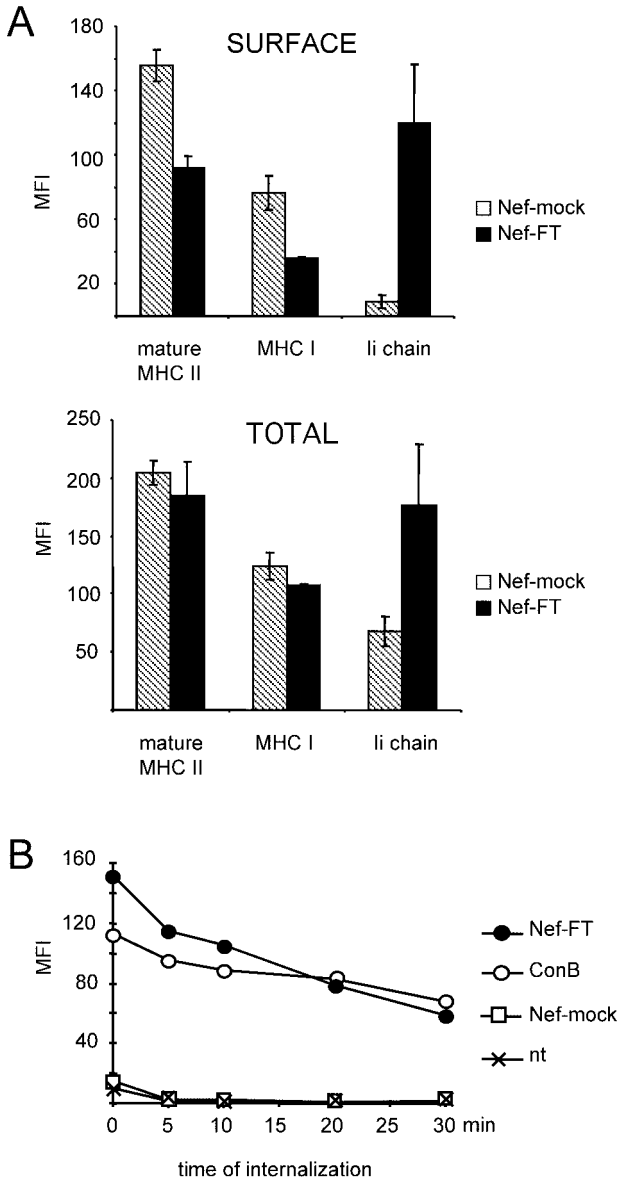

Figure 2. Nef induces intracellular accumulation of mature MHC II. (A) HeLa-CIITA cells transfected with Nef-FT or Nef-mock were stained in parallel for expression of mature MHC II, MHC I, and Ii chain either at the cell surface of intact cells or in total in permeabilized cells by using L243, W6/32, and LN-2 mAbs, respectively. MFI values of GFP$^+$ gated cells were determined for the indicated markers in FL-2. The background MFI value (obtained with a control mAb) was subtracted from these MFI values, which were then represented for the indicated molecules. (B) HeLa-CIITA cells transfected 24 h earlier with either Nef-FT or Nef-mock and pEGFP, or nontransfected cells previously exposed to 20 nM ConB, were collected and incubated with an anti-Ii antibody for 30 min on ice. After washes, cells were chased at 37°C for the indicated period of time, at the end of which eventual surface antibodies were revealed with secondary antibodies labeled with PE. Analysis by FACS of PE-fluorescence of GFP$^+$ cells was performed (except in the case of ConB-treated cells, where all cells were analyzed). MFIs are plotted as a function of time of internalization.

Surface Immature MHC II Are Delayed on Their Way to Lysosomal Compartments after Internalization in Nef-expressing Cells

To follow the fate of $\alpha\beta$Ii complexes after their internalization, HeLa-CIITA cells transfected with Nef-FT or with Nef-mock were incubated first for 60 min at 19.5°C in the presence of appropriate anti-Ii antibodies. At this temperature, endocytosed material is blocked in the early endosome in HeLa cells (Dunn *et al*., 1980; Mallard *et al*., 1998). Cells were then washed and chased at 37°C for 90 min before fixation, permeabilization, and staining with labeled secondary antibodies to reveal the internalized antibodies. Using this procedure, even control cells internalized detectable levels of mAb despite their low level of surface Ii. We first established by three-color confocal microscopy analysis that only transfected cells, expressing GFP and Nef, were heavily labeled with internalized anti-Ii mAb. The latter mainly consisted of a vesicular staining, concentrated in a perinuclear area where it partially but significantly codistributed with Nef but not with TGN46 (Figure 3A). In Nef-expressing cells, internalized anti-Ii mAb poorly codistributed with lysosomal/acidic structures labeled with LysoTracker (Figure 3B) or with antibodies specific for Lamp-1, despite the long chase time used. In contrast, in Nef-mock transfected cells, a significant codistribution of stainings was observed (Figure 3B), showing that the antibodies bound to the Ii chain can reach acidic compartments and remain detectable. Note that in control cells, both markers localized in small dots scattered all over the cells, whereas in cells expressing Nef, they were retained in larger but distinct structures polarized on one side of the cells (Figure 3). Additional stainings were performed under similar conditions, by using TfR-specific mAb instead of LysoTracker (Figure 3B) or by exposing cells to Tf-Cy3 for 1 h. Both procedures gave identical results. As expected in control cells, no codistribution was seen, indicating that anti-Ii chain antibodies and probably the Ii-containing complexes had left TfR^+ compartments to reach lysosomes. In contrast, in Nef-expressing cells both markers exhibited a partial codistribution in a perinuclear area (Figure 3B). Finally, the use of rab11-specific antibodies in Nef-expressing cells resulted in very limited colocalization with internalized anti-Ii antibodies (our unpublished data). These data suggest that in the presence of Nef, internalized anti-Ii antibodies, and therefore probably Ii chain-containing complexes are delayed on their way to lysosomal compartments and accumulate in perinuclear compartments, partially colocalizing with TfR^+ structures.

Nef Effect on Transport to Lysosomes

To further establish the Nef-induced delay in transport of immature MHC II to lysosomes and to evaluate the specificity of this inhibition, subcellular fractionation experiments were carried out. Such biochemical analysis requires homogenous cell populations expressing Nef. For this purpose, we made a recombinant adenovirus encoding Nef-Ires-HA (see MATERIALS AND METHODS). The HA protein can be detected by FACS at the cell surface of infected cells, and these HA-positive cells also express Nef. Cells infected with a virus encoding HA alone were used as controls. Infection efficiency exceeded 90% in both cell populations as judged by HA expression monitored by FACS. The Nef-induced modifications of cell surface markers such as Ii and MHC I and II were checked in parallel and gave results similar to the ones depicted in Figure 2A. Control and Nef-expressing cells were disrupted using a ball-bearing homogenizer, and their postnuclear supernatants were subjected to Percoll density gradient fractionation. Western blotting of the fractions showed that this procedure successfully separated light organelles such as the endoplasmic reticulum (ER) from heavy ones such as lysosomes. ER-containing fractions (number 10–15) were identified using calreticulin and Erp57-specific antibodies (our unpublished data). Lysosome-containing fractions (number 2–5) were identified by monitoring β-hexosaminidase activity and reactivity for Lamp-1 and HLA-DMβ-specific antibodies. In control cells, MHC II was distributed in two peaks. The first one (fractions 10–15) is probably composed of MHC II associated with plasma membrane, endosomes as well as ER membranes. The second one (fractions 2–5) is enriched in lysosomes. Nef expression profoundly modified the distribution of Ii and MHC II chains. In the presence of Nef, dense fractions contained much lower levels (almost undetectable) of Ii chain and lower amounts of MHC II. In light fractions the reverse was true, i.e., both Ii chain and MHC II levels were increased compared with control cells. As previously observed (Stumptner-Cuvelette *et al*., 2001) and in agreement with the pulse-chase experiments (Figure 1), the total amount of Ii chain found in Nef-expressing cells was much higher than in control cells (Figure 4). In contrast, Nef expression did not alter the distribution of Lamp-1, HLA-DMβ, and β-hexosaminidase (Figure 4), indicating that protein transport to lysosomes normally occurs in the presence of Nef. This conclusion is supported by our observation that EGF degradation was not affected by Nef expression (Johannes *et al*., 2003).

Together, our data suggest that Nef expression leads to a specific inhibition of transport to lysosomal compartments of $\alpha\beta$Ii complexes.

Nef-expressing Cells Accumulate MVBs

To gain insights into the Nef-induced modifications of the endocytic pathway, we performed immunogold labeling on ultrathin cryosections of Nef or mock-transfected HeLa-CIITA cells. Nef labeling was mainly associated with intracellular membranes, such as the inner face of the plasma membrane (our unpublished data), in the Golgi area, and all along endosomal compartments (Figure 5). The association of Nef with tubulovesicular elements in the TGN area seemed particularly evident (Figure 5) and might be related to the capacity of Nef to interact with AP-1 and PACS-1 complexes. Interestingly, Nef labeling was often observed at the limiting membrane of MVBs (Figure 5, top inset) and also in tubulovesicular structures closely apposed to these organelles (Figure 5, bottom inset). These elements often exhibited electron-dense areas suggestive of cytosolic coats (Figure 5, arrow, bottom inset). Nef expression did not affect the morphology of the Golgi apparatus (Figure 5) but induced a striking accumulation of MHC II-positive multivesicular endosomes or MVBs (Figure 6). These MVBs were often accumulated near the nucleus (our unpublished data) and were distinct from the Lamp-1-positive lysosomal compartments containing both internal vesicles and multilaminar membranes (Figure 6, B and C). Our immunoelectron microscopy observations indicated that in the presence of Nef, MVBs were more abundant compared with lysosomes than in mock-transfected cells. Moreover, they often seemed increased in size (with a diameter up to 700 nm, whereas in control cells it is closer to 300 nm) and contained tightly packed intralumenal vesicles (Figures 6 and 8). We have therefore estimated the numbers of MVBs and lysosomes (defined on the basis of their morphological appearance and

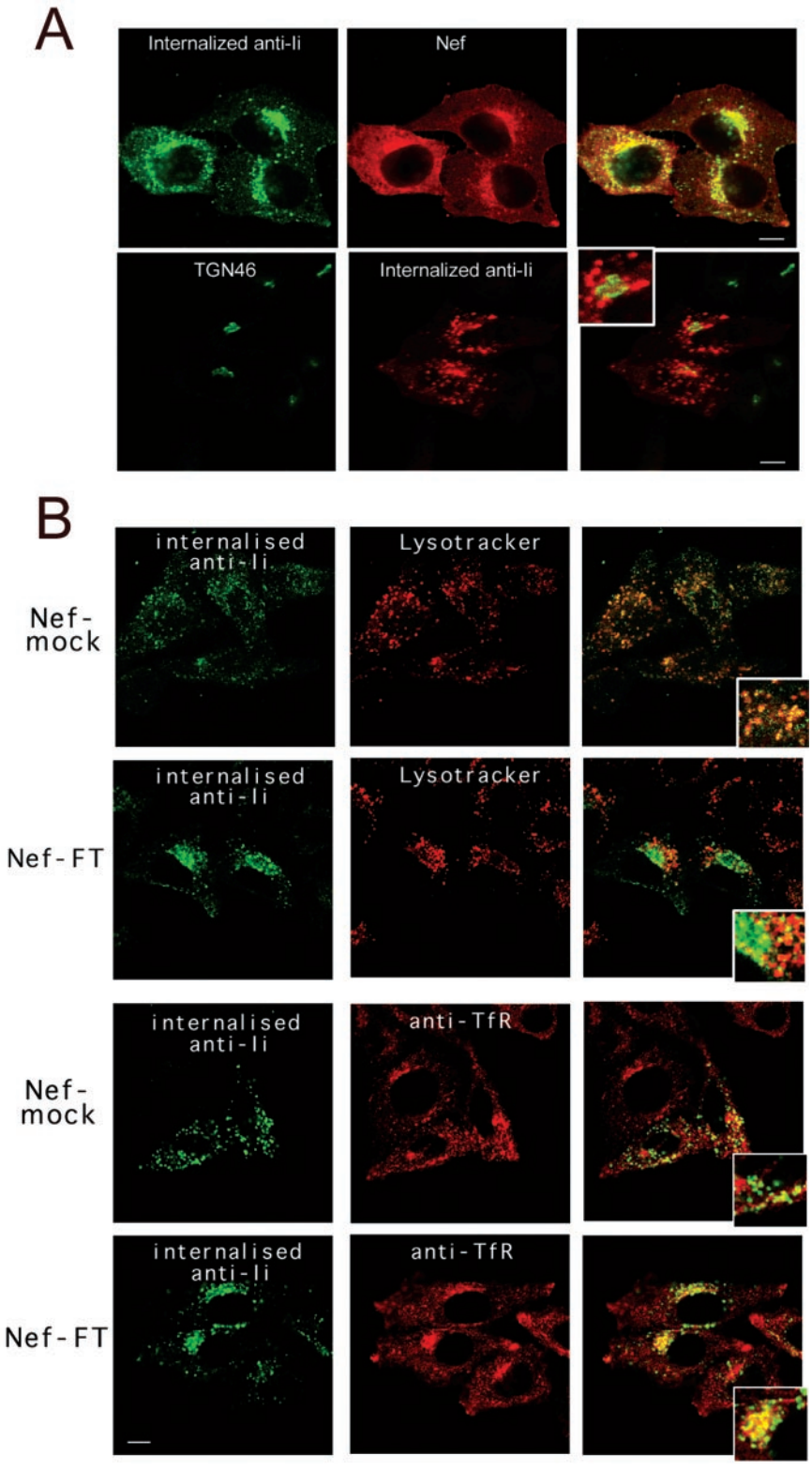

Figure 3. Nef expression impedes access of internalized immature MHC II complexes to lysosomal compartments. Confocal microscopy of HeLa-CIITA cells transfected with Nef-mock or Nef-FT. Confocal sections of the indicated stainings are presented together with their overlays that contain an insert representing a higher magnification of the same field. Bars, 10 μm. (A) Cells were incubated with either rabbit (top row) or mouse (bottom row) anti-Ii chain antibodies for 1 h at 19.5°C and then chased for 90 min at 37°C. After washes and fixation, remaining anti-Ii antibodies were revealed with appropriate FITC-labeled secondary antibodies. Cells were costained with either the anti-Nef mAb FMATG-Cy3 or with a sheep anti-TGN46 immunosera revealed by Cy3-labeled secondary antibodies. Nef and anti-Ii chain stainings clearly overlap in the top row. Although very close, TGN46 and Ii chain specific antibodies do not colocalize in Nef-expressing cells, note the magnification in the inset. (B) Two upper rows: cells were incubated for 1 h at 19.5°C with the anti-Ii mAb LN-2, washed, and chased for 90 min at 37°C in the presence of LysoTracker, which labels acidic compartments in red. Remaining LN-2 was revealed with FITC-labeled secondary antibodies. Note the abundant colocalization of both stainings in control cells (Nef-mock). Nef-transfected cells can be easily identified by the increased amount of internalized anti-Ii antibody, which reaches acidic compartments to a much lesser extent than in control cells. Two lower rows: transfection and internalization were carried out as described above except for the use of rabbit anti-Ii immune serum revealed by FITC-labeled anti-rabbit antibodies. Cells were costained with an anti-TfR mAb revealed by Cy3-labeled secondary antibodies. Anti-Ii antibodies codistribute partially with TfR in cells transfected with Nef-FT and to a much lower extent in control cells.

content; Figure 6) in Nef-expressing HeLa-CTIIA and Mel JuSo cells compared with control cells (Figure 7). In both cell lines, Nef expression induced a substantial and similar increase in the numbers of MVBs compared with the numbers of lysosomes. These MVBs contained MHC II and CD63, which is a classical marker for late endosomes also present in MHC II-rich compartments (Figure 8A). Invariant chain detected by cytosolic-specific (ICN1) or lumenal-specific (ICC5) antibodies was also abundant in these MVBs (Figure 8, B and C, respectively). ICC5 antibodies decorated ~10%

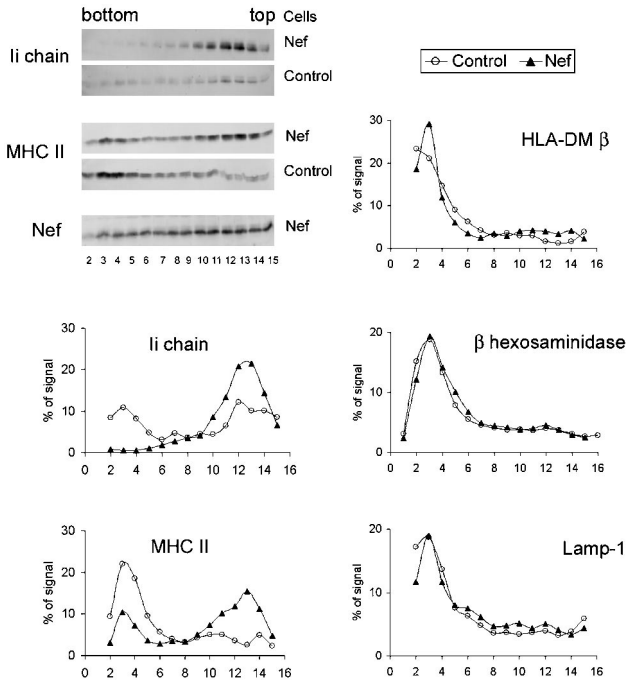

Figure 4. Specificity of Nef effect on transport to lysosomal compartments. HeLa-CIITA cells infected 24 h earlier with Ad-HA or with Ad-Nef-IRES-HA were disrupted by a ball-bearing homogenizer and fractionated on a Percoll density gradient. Aliquots of each fraction were analyzed by SDS-PAGE followed by immunoblotting for expression of HLA-DMβ (with HLA-DM-K8 mAb), Lamp-1 (with anti-Lamp-1 mAb), Invariant chain (with rabbit anti-Ii immunoserum), HLA-DRα (with 1B5 mAb) and Nef (FMATG 20 mAb). In the top left corner, Western blots of Ii, HLA-DRα, and Nef are presented. In parallel, β-hexosaminidase activity was measured in each fraction. Histogram quantifications of the indicated proteins are presented for both cell populations. The heavy fractions of both cell types contained similar levels of β-hexosaminidase activity and of HLA-DMβ and Lamp-1 proteins. Compared with control cells, Nef-expressing cells contained higher amounts of Ii chain and HLA-DRα chains in their light fractions, whereas lesser amounts of both chains were detected in their heavy fractions.

of the MVBs in control cells, whereas the majority of the MVBs were positive for ICC5 in Nef-expressing cells. Moreover, Ii chain seemed more concentrated on internal vesicles than on the limiting membrane (Figure 8, B and C). In agreement with FACS and biochemical data, Ii chain was clearly seen by immuno-EM at the plasma membrane of Nef-expressing cells (our unpublished data). Finally, access of BSA-gold, a marker of fluid phase endocytosis to these compartments was monitored. Cells transfected with Nef-FT or Nef-mock were exposed to BSA-gold for 2 h at 37°C. BSA-gold was detected in the Nef-induced MVBs, further confirming their endocytic origin (Figure 8C). However, the number of gold particles per compartment was smaller in Nef-expressing cells, possibly due to the increased number of MVBs. Accumulation of LysoTracker during 1 h at 37°C measured by FACS (Stumptner-Cuvelette *et al*., 2001), as well as accumulation of the weak base DAMP measured by immuno-EM, were comparable in cells expressing Nef versus control cells (our unpublished data), indicating that acidification of the endosomal pathway was not affected by Nef expression.

We concluded that Nef expression induced a strong increase in the number of MVBs, which were filled with numerous internal vesicles. These MVBs belong to the endocytic pathway because they were accessible to a marker of fluid phase endocytosis. Finally, the MVBs were surrounded by Nef, seemed to contain high amounts of Ii chain and MHC II and thus may represent the location, where immature and mature MHC II complexes accumulate in the presence of Nef.

Nef-induced Up-Regulation of Surface Ii Chain Is Inhibited by LY294002 Exposure

Proteins that regulate intracellular trafficking and that interact with Nef are candidates for cellular effectors of Nef. Interestingly, Nef has been shown to be able to bind and activate a PI 3-kinase (Schibeci *et al*., 2000; Wolf *et al*., 2001; Linnemann *et al*., 2002). This enzyme is involved in Nef-induced down-regulation of MHC I (Swann *et al*., 2001; Blagoveshchenskaya *et al*., 2002). To test whether a PI 3-kinase is involved in Nef's effect on MHC II, we treated Nef-

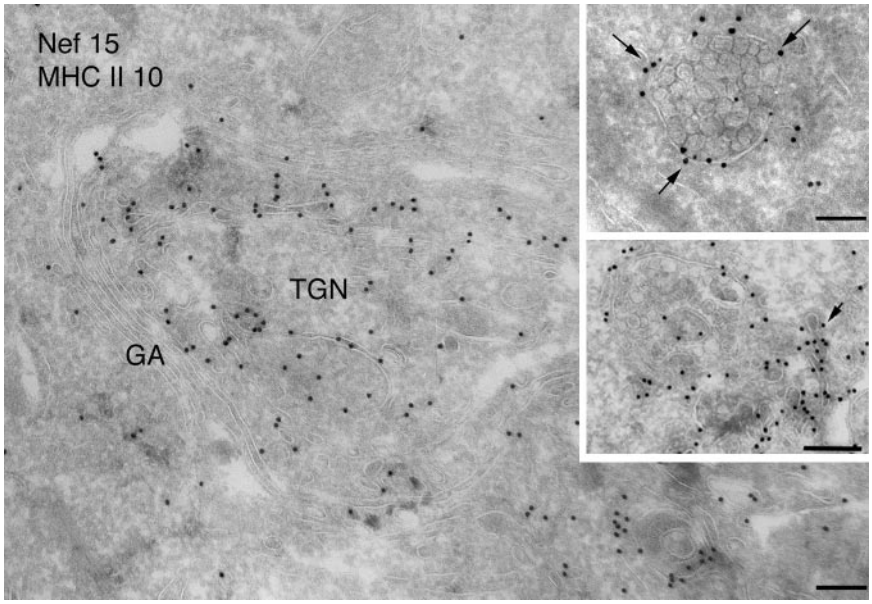

Figure 5. Immunoelectron microscopy analysis of Nef-expressing cells. Ultrathin cryosections of HeLa-CIITA cells transfected with Nef-FT were double immunogold-labeled with the anti-Nef mAb MATG (protein A gold [PAG] 15) and the anti-DR polyclonal antibody (PAG 10). Bar, 200 nm. Nef is associated with numerous membrane vesicles and tubulovesicular elements at the TGN. The Nef protein is also associated with the cytosolic side of the limiting membrane of MVB (top inset, arrows) and closely apposed tubulovesicular structures (bottom inset) that are often coated (see arrow). Bar (insets), 100 nm.

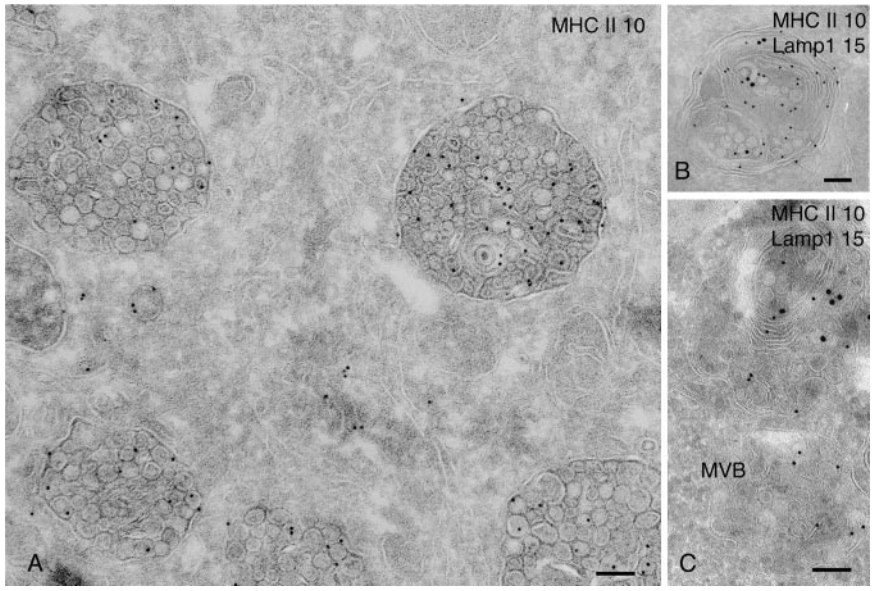

Figure 6. Nef-expressing cells accumulate MVBs. (A) Ultrathin cryosections of HeLa-CIITA cells transfected with Nef-FT were single immuno-gold labeled with antibodies directed against HLA-DR (PAG 10). This micrograph shows two typical MHC II^+ MVBs observed in Nef-expressing cells with tightly packed internal vesicles. (B) Lysosomes in HeLa-CIITA cells transfected with Nef-FT display multilaminar membranes and contain Lamp-1 (PAG 15) and MHC II (PAG 10). (C) Ultrathin cryosection of mock-transfected HeLa-CIITA cells were double immunogold labeled for Lamp-1 (PAG 15) and MHC II (PAG 10). Note the MVB immunogold labeled only for MHC II (MVB) and lysosomes containing both MHC II and Lamp-1. Bar, 100 nm.

or mock-transfected HeLa-CIITA cells with LY294002, a specific inhibitor of PI 3-kinases. This agent blocked the ability of Nef to induce Ii chain surface expression but had no effect on Nef's effects on mature MHC II nor on MHC I as assayed by flow cytometry (Figure 9A). This latter result is in agreement with the published observation that Nef induces down-regulation of HLA-A2 is inhibited by LY294002 in T cells and astrocytic cells but not in HeLa cells (Kasper and Collins, 2003). The modifications induced by the inhibitor were further examined on samples stained for Ii chain and examined by immunofluorescence (Figure 9B). As previously shown in Mel JuSo cells (Fernandez-Borja *et al*., 1999), LY294002 exposure of control cells induced large vacuoles. Ii chain staining became exclusively concentrated in these vacuoles. Nef-expressing cells treated with DMSO showed the expected Ii chain surface staining, whereas LY294002 exposure drastically reduced Ii chain surface staining, which seemed concentrated in intracellular compartments of intermediate size. Confirming our previous mutational analysis of Nef effects, these data indicate that effects of Nef on mature and immature MHC II probably involve different cellular effectors. The PI 3-kinase activated by Nef seems to be required for the effects of Nef on Ii chain and therefore on immature MHC II.

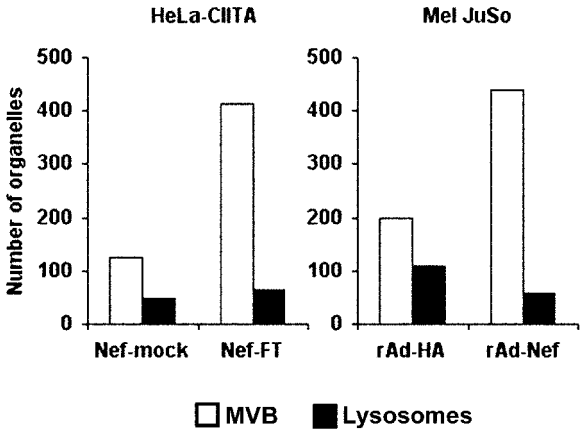

Figure 7. Nef-expressing cells accumulate MVBs. HeLa-CIITA cells were transfected with Nef-mock or Nef-FT. Mel JuSo cells were infected with recombinant adenovirus encoding either Nef and HA (here noted rAd-Nef) or HA (rAd-HA) (see MATERIALS AND METHODS). The numbers of MVBs and lysosomes in each cell type were counted directly under the electron microscope on ultrathin cryosections immunogold labeled for Nef.

DISCUSSION

Nef is expressed early after HIV entry even before integration of the viral genome and throughout the viral cycle (Wu and Marsh, 2001). One of the many effects of Nef is to modulate cell surface expression of important immunoreceptors. In the presence of Nef, peptide presentation by MHC II is impaired (Stumptner-Cuvelette *et al*., 2001). Here, we have followed the intracellular trafficking of MHC II in Nef-expressing cells to understand the cellular events causing the Nef-induced down-regulation of mature MHC II ($\alpha\beta$-peptide) and up-regulation of immature MHC II ($\alpha\beta$Ii). Nef expression did not affect the rate of synthesis of the MHC II α, β and Ii chains, indicating that it exerts its effects at a posttranslational level. Regarding $\alpha\beta$Ii immature complexes, metabolic pulse-chase analysis combined with surface biotinylation experiments, showed that Nef expression 1) increases access of $\alpha\beta$Ii complexes at the cell surface and 2) delays Ii chain degradation. $\alpha\beta$-peptide complexes accumulated intracellularly in the presence of Nef as shown by cytometry on permeabilized cells, but pulse-chase analysis failed to reveal any significant inhibition of the generation of SDS-stable complexes. Antibody internalization experiments suggest that surface $\alpha\beta$Ii are internalized in the presence of Nef but cannot reach lysosomes. This interpretation is supported by results from subcellular fractionation experiments showing that in the presence of Nef, dense lysosomal-enriched fractions contained low levels of Ii chain, whereas the levels of three other lysosomal proteins remained unchanged. Compared with control cells, Nef-expressing cells contained larger amounts of Ii chain, which were rather distributed in light fractions. Therefore, Nef's

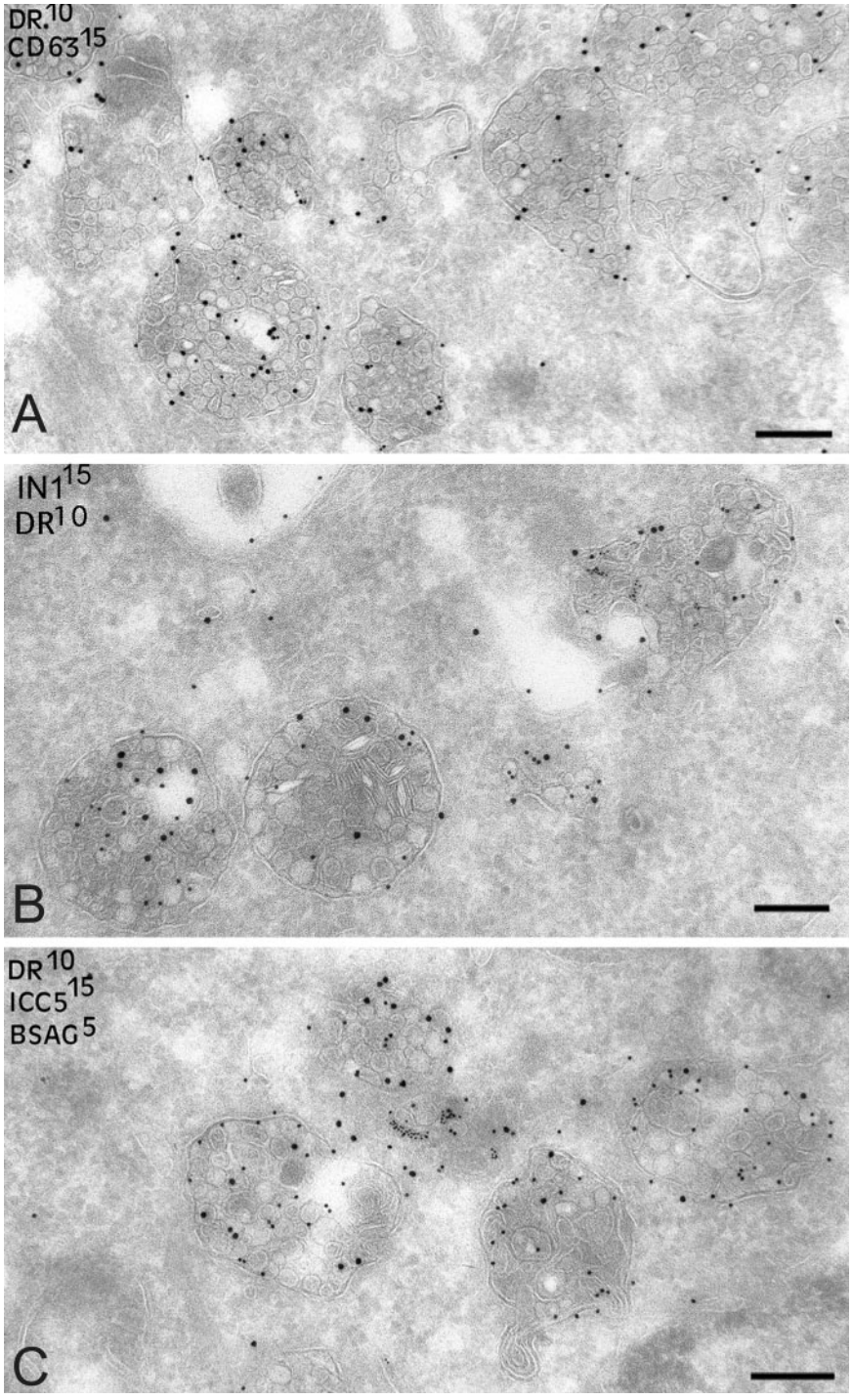

Figure 8. Accumulated MVBs in Nef-expressing cells contain CD63, MHC II, and Ii chain. Ultrathin cryosections of HeLa-CIITA cells transfected with Nef-FT were double labeled with anti-HLA-DR antibodies (protein A gold [PAG] 10) and (A) an anti-CD63 mAb (PAG 15), (B) anticytoplasmic tail of the Ii chain (PAG 15) and (C) antilumenal side of the Ii chain antibodies (PAG 15). In addition, cryosections on C were prepared from cells transfected with Nef-FT and incubated with BSA coupled to 5-nm colloidal gold for 90 min at 37°C and then fixed. Numerous multivesicular compartments accumulate in Nef-expressing cells that contain MHC II, CD63, and intact Ii chain and were accessible to internalized BSA-gold. Bar, 200 nm.

effects on $\alpha\beta$Ii complexes specifically lead to both an increased cell surface expression of $\alpha\beta$Ii, as documented previously (Stumptner-Cuvelette *et al*., 2001), and limited access of these complexes to lysosomes (this study).

Newly synthesized $\alpha\beta$Ii complexes are sorted at the level of the TGN toward the endocytic pathway (Hiltbold and Roche, 2002). This sorting step relies on signals carried by the Ii cytoplasmic tail, which also function as endocytosis signals. However, depending on the cell type considered, a variable fraction of newly synthesized $\alpha\beta$Ii complexes rapidly transits via the cell surface, is internalized, and thereby reaches the endocytic pathway (Roche *et al*., 1993; Benaroch *et al*., 1995; Saudrais *et al*., 1998; Davidson, 1999). In our cell system, low expression levels of cell surface Ii chain in control cells prevented accurate determination of the rate of endocytosis in this cell population. Nef expression does not affect endocytosis in general, because internalization of Tf (Foti *et al*., 1997), the B subunit of the Shiga toxin (Johannes *et al*., 2003) and the TfR were not modified by Nef, nor acidification of the endosomal pathway (Stumptner-Cu-

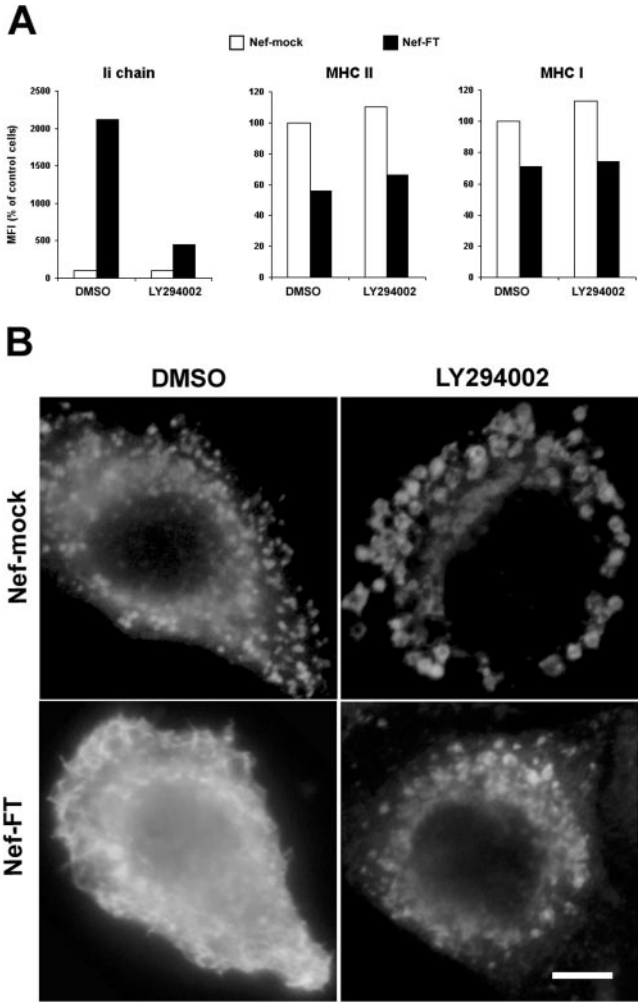

Figure 9. PI 3-kinase activity is required for the Nef-induced up-regulation of Ii chain at the cell surface. HeLa-CIITA cells were transfected with either Nef-FT or Nef-mock and pEGFP. (A) Cells were recovered 24 h posttransfection, stained, and analyzed by FACS. For the last 15 h, cells were either treated with 50 μM LY294002 or with its solvent, DMSO. For each cell population, MFI values obtained for the indicated surface marker in GFP^+ cells are represented. Data are representative of four independent experiments. (B) Localization of Ii chain by immunofluorescence microscopy. Twenty-four hours after transfection, cells were fixed, permeabilized, and stained with rabbit anti-Ii chain polyclonal antibody revealed by Cy-3–labeled secondary antibodies. For the last 3 h, cells were either treated with 50 μM LY294002 or with its solvent, DMSO. Only Cy-3 staining of transfected cells are shown (transfected cells were identified by GFP expression). Bar, 10 μM.

velette *et al*., 2001; this study). We also confirmed that in our cell system, Nef expression did not affect uptake of lucifer yellow (Foti *et al*., 1997), a marker of fluid phase endocytosis, nor dextran-FITC (40 kDa) or mannosylated-BSA-FITC (our unpublished data).

In Nef-expressing cells, surface bound anti-Ii antibodies were internalized but delayed in reaching late acidic compartments labeled with LysoTracker or anti-Lamp mAb. The anti-Ii antibodies accumulated in vesicular compartments that were negative for TGN46 and Lamp-1, and concentrated in a perinuclear area. There was some overlap between endocytosed anti-Ii antibodies and TfR, whereas the extent of the overlap was larger with Nef. These observations further illustrate the Nef-induced alterations of the endocytic pathway at the dynamic level. We also analyzed these alterations at the steady state by immuno-EM. Our analysis reveals that Nef expression induces an increase in size and number of MVBs. We estimated MVB numbers by comparison with the number of lysosomes encountered in randomly chosen ultrathin cryosections of control and Nef-expressing HeLa-CIITA cells. Nef expression induced a significant increase (almost a threefold factor) of the numbers of MVBs compared with those of lysosomes. We observed a similar Nef-induced accumulation of MVBs in the Mel JuSo melanoma cell line. As expected for such compartments, the MVBs observed in Nef-expressing cells contained internal vesicles positively labeled for CD63 and were accessible to the endocytic tracer BSA-gold after 20 min at 37°C. Antibodies specific for MHC II and Ii chain heavily decorated these compartments, whose limiting membrane was rich in the Nef protein. An unusual high reactivity with antibodies directed against the lumenal part of the Ii chain was associated with these MVBs, suggesting that in the presence of Nef large amounts of intact Ii chain have reached these compartments. Exposure of Nef expressing cells to an anti-Ii mAb led to its internalization from the surface and its access to MVBs (our unpublished data). The accumulation of MVBs observed at the EM level near the nucleus might therefore correspond to the large vesicular structures labeled with internalized anti-Ii chain antibodies and observed by confocal microscopy in Nef-expressing cells. Each vacuolar structure observed by confocal microscopy may thus correspond to several MVBs concentrated in a restricted area. Together, our data suggest that Nef induces an accumulation of MVBs where immature and mature MHC II complexes accumulate. By preventing $\alpha\beta$Ii access to lysosomal compartments rich in proteases, Ii chain degradation would be reduced. Cysteine proteases are involved in Ii chain degradation in the endocytic pathway. We analyzed the cysteine protease activity present in total lysates from Nef-expressing cells compared with control cells by using an active site-directed probe (Lennon-Dumenil *et al*., 2002). We did not find any significant difference (our unpublished data), suggesting that Nef does not affect cysteine protease activity in general. This conclusion is supported by our observation that EGF degradation normally occurs in Nef-expressing cells (Johannes *et al*., 2003).

Strikingly, the effects of Nef expression on MVBs seem opposite to the effects induced by the PI 3-kinase inhibitors wortmannin and LY294002 (Fernandez-Borja *et al*., 1999). Indeed, exposure of MHC II-expressing cells to PI 3-kinase inhibitors induces swelling of MVBs, which contain much less internal vesicles. Moreover, Nef is known to bind and activate a PI 3-kinase (Schibeci *et al*., 2000; Wolf *et al*., 2001; Linnemann *et al*., 2002), which is involved in Nef-induced MHC I down-regulation (Swann *et al*., 2001; Blagoveshchenskaya *et al*., 2002). We therefore tested the possible involvement of PI 3-kinase in the Nef-induced effects on MHC II. We observed that exposure of Nef-expressing cells to LY294002 abolished Nef-induced up-regulation of Ii chain at the cell surface as estimated by FACS and by immunofluorescence. In contrast, the inhibitor had no effect on Nef-induced down-regulation of surface mature MHC II and MHC I. These data support our previous conclusion based on mutational analysis that Nef acts through different mechanisms on mature and immature MHC II (Stumptner-Cuvelette *et al*., 2001). In addition, these data suggest that the increased surface expression of $\alpha\beta$Ii induced by Nef in-

volves a PI 3-kinase activity sensitive to LY294002. Phosphoinositides produced by PI 3-kinases direct the localization and the activity of effector proteins critical for cellular transport processes such as endocytosis and biosynthetic trafficking (Odorizzi *et al*., 2000; Simonsen *et al*., 2001). Thus, Nef could increase the access of $\alpha\beta$Ii complexes at the cell surface either from endosomes or from the TGN, via a PI 3-kinase–dependent pathway. Interestingly, several studies indicate that a PI 3-kinase activity is involved in controlling a recycling route from endosomes to the plasma membrane (Spiro *et al*., 1996; Siddhanta *et al*., 1998; Hunyady *et al*., 2002). In HeLa cells, this PI 3-kinase–dependent pathway rapidly occurs for the TfR from sorting endosomes and bypasses recycling endosomes (van Dam *et al*., 2002). However, we previously showed that Tf endocytosis and recycling are not affected by Nef expression (Johannes *et al*., 2003), indicating that recycling from sorting endosomes is not particularly active in Nef-expressing cells. In addition, recycling from late compartments, including MVBs, was also reported to be dependent on a wortmannin-sensitive PI 3-kinase activity in fibroblast cells (Bright *et al*., 2001). We localized at the ultrastructural level Nef in different compartments but a great proportion of the immunogold labeling was associated with MVB outer membrane. Nef could recruit a PI 3-kinase at this location and thus induce a local production of phosphoinositides, which have been shown to play a key role in the inward budding of MVBs and consequently, in MVB biogenesis (Simonsen *et al*., 2001; Katzmann *et al*., 2002). Therefore, the Nef-induced increase in MVB numbers might be related to the activation of a PI 3-kinase by Nef. Finally, the Nef-mediated activation of the PI 3-kinase could promote recycling of $\alpha\beta$Ii complexes to the cell surface due to their accumulation in MVBs and in agreement with their reduced capacity to access lysosomes. However, more work is required to estimate whether these hypotheses are correct.

One of the many consequences of Nef's presence is a major remodeling of the endocytic pathway as documented by this study. The significance of this modification in regard to the viral cycle is still unknown. We recently reported that in HIV-1–infected macrophages, HIV assembly seems to occur at the limiting membrane of MVB compartments, rich in MHC II (Raposo *et al*., 2002). After they pinch off, the newly formed virus particles accumulate in the lumen of these MVBs, which can fuse with the plasma membrane, releasing their viral content to the extracellular medium. This assembly process explains the particular composition of the HIV membrane, which is enriched in certain lipids such as (PI3)P (phosphatidylinositol 3-phosphate) and in host proteins such as MHC II and CD63. A very recent study has further established these points showing that in primary macrophages most of infectious HIV-1 indeed assembles in late endosomes (Pelchen-Matthews *et al*., 2003). In addition, it is now recognized that the late domain of Gag from many retroviruses, including HIV, is able to recruit the MVB machinery for viral assembly, budding, and fission processes. Mimicking Hrs during vesicles formation in MVBs, Gag late p6 domain assembles in oligomeric and monoubiquitinated complexes, which are then recognized by Tsg101, thereby initiating the assembly process (Pornillos *et al*., 2002). In T cells, this recruitment seems to occur at the plasma membrane in raft-enriched microdomains. In this respect, it is important to note that Nef not only associates with rafts (Wang *et al*., 2000) but also increases infectivity of HIV through this association, promoting incorporation of the ganglioside GM1 in the viral membrane (Zheng *et al*., 2001). Moreover, Nef-induced down-regulation of surface envelope results in its transport to the endocytic pathway (Schwartz *et al*., 1993). Therefore, HIV-1 infection may lead to the accumulation of viral and nonviral proteins in endosomal compartments. We propose that the remodeling of the endocytic pathway induced by Nef expression reflects the role of Nef in the viral program for viral assembly. There is no doubt that future studies on Nef, a small but very gifted protein, will go on providing exciting insights into the biology of host–virus interactions.

ACKNOWLEDGMENTS

We thank S. Amigorena for helpful discussions, P. Lehner for critical reading of the manuscript, S. Morchoisne and C. Dousset for technical help, A.M. Lenon-Dumesnil for help in the active site probe labeling experiments, and E. Morillon for help in making recombinant adenovirus. P.S.-C. was a fellow of Agence Nationale de recherche contre le SIDA. This work was supported by grants to P.B. from the Association dela Recherche contre le Cancer, the Agence Nationale deRecherche contre le Sida and Ensemble Contre le SIDA.

REFERENCES

Adams, T.E., Bodmer, J.G., and Bodmer, W.F. (1983). Production and characterization of monoclonal antibodies recognizing the alpha-chain subunits of human ia alloantigens. Immunology *50*, 613–624.

Aiken, C., Konner, J., Landau, N.R., Lenburg, M.E., and Trono, D. (1994). Nef induces CD4 endocytosis: requirement for a critical dileucine motif in the membrane-proximal CD4 cytoplasmic domain. Cell *76*, 853–864.

Bachelerie, F., Alcami, J., Hazan, U., Israel, N., Goud, B., Arenzana-Seisdedos, F., and Virelizier, J.L. (1990). Constitutive expression of human immunodeficiency virus (HIV) nef protein in human astrocytes does not influence basal or induced HIV long terminal repeat activity. J. Virol. *64*, 3059–3062.

Benaroch, P., Yilla, M., Raposo, G., Ito, K., Miwa, K., Geuze, H.J., and Ploegh, H.L. (1995). How MHC class II molecules reach the endocytic pathway. EMBO J. *14*, 37–49.

Blagoveshchenskaya, A.D., Thomas, L., Feliciangeli, S.F., Hung, C.H., and Thomas, G. (2002). HIV-1 Nef downregulates MHC-I by a PACS-1- and PI3K-regulated ARF6 endocytic pathway. Cell *111*, 853–866.

Bonnerot, C., Briken, V., Brachet, V., Lankar, D., Cassard, S., Jabri, B., and Amigorena, S. (1998). syk protein tyrosine kinase regulates Fc receptor gamma-chain-mediated transport to lysosomes. EMBO J. *17*, 4606–4616.

Bright, N.A., Lindsay, M.R., Stewart, A., and Luzio, J.P. (2001). The relationship between lumenal and limiting membranes in swollen late endocytic compartments formed after wortmannin treatment or sucrose accumulation. Traffic *2*, 631–642.

Chartier, C., Degryse, E., Gantzer, M., Dieterle, A., Pavirani, A., and Mehtali, M. (1996). Efficient generation of recombinant adenovirus vectors by homologous recombination in *Escherichia coli*. J. Virol. *70*, 4805–4810.

Cohen, G.B., Gandhi, R.T., Davis, D.M., Mandelboim, O., Chen, B.K., Strominger, J.L., and Baltimore, D. (1999). The selective downregulation of class I major histocompatibility complex proteins by HIV-1 protects HIV-infected cells from NK cells. Immunity *10*, 661–671.

Collins, K.L., and Baltimore, D. (1999). HIV's evasion of the cellular immune response. Immunol. Rev. *168*, 65–74.

Collins, K.L., Chen, B.K., Kalams, S.A., Walker, B.D., and Baltimore, D. (1998). HIV-1 Nef protein protects infected primary cells against killing by cytotoxic T lymphocytes. Nature *391*, 397–401.

Davidson, H.W. (1999). Direct transport of newly synthesized HLA-DR from the trans-Golgi network to major histocompatibility complex class II containing compartments (MIICS) demonstrated using a novel tyrosine-sulfated chimera. J. Biol. Chem. *274*, 27315–27322.

Dorfman, T., Popova, E., Pizzato, M., and Gottlinger, H.G. (2002). Nef enhances human immunodeficiency virus type 1 infectivity in the absence of matrix. J. Virol. *76*, 6857–6862.

Dunn, W.A., Hubbard, A.L., and Aronson, N.N., Jr. (1980). Low temperature selectively inhibits fusion between pinocytic vesicles and lysosomes during heterophagy of 125I-asialofetuin by the perfused rat liver. J. Biol. Chem. *255*, 5971–5978.

Fackler, O.T., and Baur, A.S. (2002). Live and let die: Nef functions beyond HIV replication. Immunity *16*, 493–497.

Fernandez-Borja, M., Wubbolts, R., Calafat, J., Janssen, H., Divecha, N., Dusseljee, S., and Neefjes, J. (1999). Multivesicular body morphogenesis requires phosphatidyl-inositol 3-kinase activity. Curr. Biol. *9*, 55–58.

Foti, M., Mangasarian, A., Piguet, V., Lew, D.P., Krause, K.H., Trono, D., and Carpentier, J.L. (1997). Nef-mediated clathrin-coated pit formation. J. Cell Biol. *139*, 37–47.

Garcia, J.V., and Miller, A.D. (1991). Serine phosphorylation-independent downregulation of cell-surface CD4 by nef. Nature *350*, 508–511.

Greenberg, M.E., Iafrate, A.J., and Skowronski, J. (1998). The SH3 domain-binding surface and an acidic motif in HIV-1 Nef regulate trafficking of class I MHC complexes. EMBO J. *17*, 2777–2789.

Hanna, Z., Kay, D.G., Cool, M., Jothy, S., Rebai, N., and Jolicoeur, P. (1998a). Transgenic mice expressing human immunodeficiency virus type 1 in immune cells develop a severe AIDS-like disease. J. Virol. *72*, 121–132.

Hanna, Z., Kay, D.G., Rebai, N., Guimond, A., Jothy, S., and Jolicoeur, P. (1998b). Nef harbors a major determinant of pathogenicity for an AIDS-like disease induced by HIV-1 in transgenic mice. Cell *95*, 163–175.

Hiltbold, E.M., and Roche, P.A. (2002). Trafficking of MHC class II molecules in the late secretory pathway. Curr. Opin. Immunol. *14*, 30–35.

Hunyady, L., Baukal, A.J., Gaborik, Z., Olivares-Reyes, J.A., Bor, M., Szaszak, M., Lodge, R., Catt, K.J., and Balla, T. (2002). Differential PI 3-kinase dependence of early and late phases of recycling of the internalized AT1 angiotensin receptor. J. Cell Biol. *157*, 1211–1222.

Johannes, L., Pezo, V., Mallard, F., Tenza, D., Wiltz, A., Saint-Pol, A., Helft, J., Antony, C., and Benaroch, P. (2003). Effects of HIV-1 Nef on retrograde transport from the plasma membrane to the endoplasmic reticulum. Traffic *4*, 323–332.

Kasper, M.R., and Collins, K.L. (2003). Nef-mediated disruption of HLA-A2 transport to the cell surface in T cells. J. Virol. *77*, 3041–3049.

Katzmann, D.J., Odorizzi, G., and Emr, S.D. (2002). Receptor downregulation and multivesicular-body sorting. Nat. Rev. Mol. Cell Biol. *3*, 893–905.

Kestler, H. W. d., Ringler, D.J., Mori, K., Panicali, D.L., Sehgal, P.K., Daniel, M.D., and Desrosiers, R.C. (1991). Importance of the nef gene for maintenance of high virus loads and for development of AIDS. Cell *65*, 651–662.

Lama, J., Mangasarian, A., and Trono, D. (1999). Cell-surface expression of CD4 reduces HIV-1 infectivity by blocking Env incorporation in a Nef- and Vpu-inhibitable manner. Curr. Biol. *9*, 622–631.

Lamb, C., and Cresswell, P. (1992). Assembly and transport properties of invariant chain trimers and HLA-DR-invariant chain complexes. J. Immunol. *148*, 3478–3482.

Lampson, L.A., and Levy, R. (1980). Two populations of Ia-like molecules on a human B cell line. J. Immunol. *125*, 293–299.

Le Gall, S., Erdtmann, L., Benichou, S., Berlioz-Torrent, C., Liu, L., Benarous, R., Heard, J.M., and Schwartz, O. (1998). Nef interacts with the mu subunit of clathrin adaptor complexes and reveals a cryptic sorting signal in MHC I molecules. Immunity *8*, 483–495.

Lennon-Dumenil, A.-M., Bakker, A.H., Maehr, R., Fiebiger, E., Overkleeft, H.S., Rosemblatt, M., Ploegh, H.L., and Lagaudriere-Gesbert, C. (2002). Analysis of protease activity in live antigen-presenting cells shows regulation of the phagosomal proteolytic contents during dendritic cell activation. J. Exp. Med. *196*, 529–540.

Linnemann, T., Zheng, Y.H., Mandic, R., and Matija Peterlin, B. (2002). Interaction between Nef and phosphatidylinositol-3-kinase leads to activation of p21-activated kinase and increased production of HIV. Virology *294*, 246–255.

Lundquist, C.A., Tobiume, M., Zhou, J., Unutmaz, D., and Aiken, C. (2002). Nef-mediated downregulation of CD4 enhances human immunodeficiency virus type 1 replication in primary T lymphocytes. J. Virol. *76*, 4625–4633.

Mallard, F., Antony, C., Tenza, D., Salamero, J., Goud, B., and Johannes, L. (1998). Direct pathway from early/recycling endosomes to the Golgi apparatus revealed through the study of shiga toxin B-fragment transport. J. Cell Biol. *143*, 973–990.

Miller, M.D., Warmerdam, M.T., Gaston, I., Greene, W.C., and Feinberg, M.B. (1994). The human immunodeficiency virus-1 nef gene product: a positive factor for viral infection and replication in primary lymphocytes and macrophages. J. Exp. Med. *179*, 101–113.

Munch, J., Stolte, N., Fuchs, D., Stahl-Hennig, C., and Kirchhoff, F. (2001). Efficient class i major histocompatibility complex down-regulation by simian immunodeficiency virus nef is associated with a strong selective advantage in infected rhesus macaques. J. Virol. *75*, 10532–10536.

Odorizzi, G., Babst, M., and Emr, S.D. (2000). Phosphoinositide signaling and the regulation of membrane trafficking in yeast. Trends Biochem. Sci. *25*, 229–235.

Parham, P., Barnstable, C.J., and Bodmer, W.F. (1979). Use of monoclonal antibody (W6/32) in structural studies of HLA-A, B, C antigens. J. Immunol. *123*, 342–349.

Pelchen-Matthews, A., Kramer, B., and Marsh, M. (2003). Infectious HIV-1 assembles in late endosomes in primary macrophages. J. Cell Biol. *162*, 443–455.

Piguet, V., Wan, L., Borel, C., Mangasarian, A., Demaurex, N., Thomas, G., and Trono, D. (2000). HIV-1 Nef protein binds to the cellular protein PACS-1 to downregulate class I major histocompatibility complexes. Nat. Cell Biol. *2*, 163–167.

Pitcher, C.J., Quittner, C., Peterson, D.M., Connors, M., Koup, R.A., Maino, V.C., and Picker, L.J. (1999). HIV-1-specific CD4+ T cells are detectable in most individuals with active HIV-1 infection, but decline with prolonged viral suppression [see comments]. Nat. Med. *5*, 518–525.

Pornillos, O., Garrus, J.E., and Sundquist, W.I. (2002). Mechanisms of enveloped RNA virus budding. Trends Cell Biol. *12*, 569–579.

Raposo, G., Kleijmeer, M.J., Posthuma, G., Slot, J.W., and Geuze, H.J. (1997). Immunogold labeling of ultrathin cryosections: application in immunology. In: Weir's Handbook of Experimental Immunology, 5th ed., Ch 208, ed. L.A. Herzenberg, D.M. Weir, L. Herzenberg, and C. Blackwell, Cambridge, MA: Blackwell Science, 1–11.

Raposo, G., Moore, M., Innes, D., Leijendekker, R., Leigh-Brown, A., Benaroch, P., and Geuze, H. (2002). Human macrophages accumulate HIV-1 particles in MHC II compartments. Traffic *3*, 718–729.

Roche, P.A., Teletski, C.L., Stang, E., Bakke, O., and Long, E.O. (1993). Cell surface HLA-DR-invariant chain complexes are targeted to endosomes by rapid internalization. Proc. Natl. Acad. Sci. USA *90*, 8581–8585.

Rosenberg, E.S., Billingsley, J.M., Caliendo, A.M., Boswell, S.L., Sax, P.E., Kalams, S.A., and Walker, B.D. (1997). Vigorous HIV-1-specific CD4+ T cell responses associated with control of viremia [see comments]. Science *278*, 1447–1450.

Ross, T.M., Oran, A.E., and Cullen, B.R. (1999). Inhibition of HIV-1 progeny virion release by cell-surface CD4 is relieved by expression of the viral nef protein. Curr. Biol. *9*, 613–621.

Salamero, J., Le, B.R., Saudrais, C., Goud, B., and Hoflack, B. (1996). Expression of major histocompatibility complex class II molecules in HeLa cells promotes the recruitment of AP-1 Golgi-specific assembly proteins on Golgi membranes. J. Biol. Chem. *271*, 30318–30321.

Sarukhan, A., Camugli, S., Gjata, B., von Boehmer, H., Danos, O., and Jooss, K. (2001). Successful interference with cellular immune responses to immunogenic proteins encoded by recombinant viral vectors. J. Virol. *75*, 269–277.

Saudrais, C., Spehner, D., de la Salle, H., Bohbot, A., Cazenave, J.P., Goud, B., Hanau, D., and Salamero, J. (1998). Intracellular pathway for the generation of functional M.H.C. class II peptide complexes in immature human dendritic cells. J. Immunol. *160*, 2597–2607.

Schibeci, S.D., Clegg, A.O., Biti, R.A., Sagawa, K., Stewart, G.J., and Williamson, P. (2000). HIV-Nef enhances interleukin-2 production and phosphatidylinositol 3-kinase activity in a human T cell line. Aids *14*, 1701–1707.

Schindler, M., Würfl, S., Benaroch, P., Greenough, T. C., Daniels, R., Easterbrook, P., Brenner, M., Münch, J., and Kirchhoff, F. (2003). Down-modulation of mature MHC class II and up-regulation of invariant chain cell surface expression are well conserved functions of human and simian immunodeficiency virus nef-alleles. J. Virol. *77*, 10548–10556.

Schwartz, O., Marechal, V., Danos, O., and Heard, J.M. (1995). Human immunodeficiency virus type 1 Nef increases the efficiency of reverse transcription in the infected cell. J. Virol. *69*, 4053–4059.

Schwartz, O., Marechal, V., Le Gall, S., Lemonnier, F., and Heard, J.M. (1996). Endocytosis of major histocompatibility complex class I molecules is induced by the HIV-1 Nef protein. Nat. Med. *2*, 338–342.

Schwartz, O., Riviere, Y., Heard, J.M., and Danos, O. (1993). Reduced cell surface expression of processed human immunodeficiency virus type 1 envelope glycoprotein in the presence of Nef. J. Virol. *67*, 3274–3280.

Shaw, S., Ziegler, A., and DeMars, R. (1985). Specificity of monoclonal antibodies directed against human and murine class II histocompatibility antigens as analyzed by binding to HLA-deletion mutant cell lines. Hum. Immunol. *12*, 191–211.

Siddhanta, U., McIlroy, J., Shah, A., Zhang, Y., and Backer, J.M. (1998). Distinct roles for the p110alpha and hVPS34 phosphatidylinositol 3′-kinases

in vesicular trafficking, regulation of the actin cytoskeleton, and mitogenesis. J. Cell Biol. *143*, 1647–1659.

Simonsen, A., Wurmser, A.E., Emr, S.D., and Stenmark, H. (2001). The role of phosphoinositides in membrane transport. Curr. Opin. Cell Biol. *13*, 485–492.

Spina, C.A., Kwoh, T.J., Chowers, M.Y., Guatelli, J.C., and Richman, D.D. (1994). The importance of nef in the induction of human immunodeficiency virus type 1 replication from primary quiescent CD4 lymphocytes. J. Exp. Med. *179*, 115–123.

Spiro, D.J., Boll, W., Kirchhausen, T., and Wessling-Resnick, M. (1996). Wortmannin alters the transferrin receptor endocytic pathway in vivo and in vitro. Mol. Biol. Cell *7*, 355–367.

Stumptner, P., and Benaroch, P. (1997). Interaction of MHC class II molecules with the invariant chain: role of the invariant chain (81–90) region. EMBO J. *16*, 5807–5818.

Stumptner-Cuvelette, P., and Benaroch, P. (2002). Multiple roles of the invariant chain in MHC class II function. Biochim. Biophys. Acta *1542*, 1–13.

Stumptner-Cuvelette, P., Morchoisne, S., Dugast, M., Le Gall, S., Raposo, G., Schwartz, O., and Benaroch, P. (2001). HIV-1 Nef impairs MHC class II antigen presentation and surface expression. Proc. Natl. Acad. Sci. USA *98*, 12144–12149.

Swann, S.A., Williams, M., Story, C.M., Bobbitt, K.R., Fleis, R., and Collins, K.L. (2001). HIV-1 Nef blocks transport of MHC class I molecules to the cell surface via a PI 3-kinase-dependent pathway. Virology *282*, 267–277.

Swigut, T., Shohdy, N., and Skowronski, J. (2001). Mechanism for down-regulation of CD28 by Nef. EMBO J. *20*, 1593–1604.

van Dam, E.M., ten Broeke, T., Jansen, K., Spijkers, P., and Stoorvogel, W. (2002). Endocytosed transferrin receptors recycle via distinct dynamin and phosphatidylinositol 3-kinase-dependent pathways. J. Biol. Chem. *277*, 48876–48883.

van de Rijn, M., Geurts van Kessel, A.H., Kroezen, V., van Agthoven, A.J., Verstijnen, K., Terhorst, C., and Hilgers, J. (1983). Localization of a gene controlling the expression of the human transferrin receptor to the region q12 leads to qter of chromosome 3. Cytogenet. Cell Genet. *36*, 525–531.

Wang, J.K., Kiyokawa, E., Verdin, E., and Trono, D. (2000). The Nef protein of HIV-1 associates with rafts and primes T cells for activation. Proc. Natl. Acad. Sci. USA *97*, 394–399.

Wolf, D., Witte, V., Laffert, B., Blume, K., Stromer, E., Trapp, S., d'Aloja, P., Schurmann, A., and Baur, A.S. (2001). HIV-1 Nef associated PAK and PI3-kinases stimulate Akt-independent Bad-phosphorylation to induce anti-apoptotic signals. Nat. Med. *7*, 1217–1224.

Wraight, C.J., Van Endert, P., Möller, P., Lipp, J., Ling, N.R., MacLennan, I.C.M., Koch, N., and Moldenhauer, G. (1990). Human major histocompatibility complex class II invariant chain is expressed on the cell surface. J. Biol. Chem. *265*, 5787–5792.

Wu, Y., and Marsh, J.W. (2001). Selective transcription and modulation of resting T cell activity by preintegrated HIV DNA. Science *293*, 1503–1506.

Zheng, Y., Plemenitas, A., Linnemann, T., Fackler, O.T., and Peterlin, B.M. (2001). Nef increases infectivity of HIV via lipid rafts. Curr. Biol. *11*, 875–879.